



# Eutaxial growth of hematite $\text{Fe}_2\text{O}_3$ films on perovskite $\text{SrTiO}_3$ polycrystalline substrates

Andrew M. Schultz, Yisi Zhu, Stephanie A. Bojarski, Gregory S. Rohrer, Paul A. Salvador\*

Department of Materials Science and Engineering, Carnegie Mellon University, Pittsburgh, PA 15206, USA

## ARTICLE INFO

### Article history:

Received 11 June 2013

Received in revised form 16 September 2013

Accepted 24 September 2013

Available online 2 October 2013

### Keywords:

Epitaxy

Electron backscatter diffraction

$\text{Fe}_2\text{O}_3$

Pulsed laser deposition

Eutaxy

Combinatorial substrate epitaxy

Perovskite

$\text{SrTiO}_3$

## ABSTRACT

The grain-by-grain orientation relationships between an  $\text{Fe}_2\text{O}_3$  film, grown using pulsed laser deposition, and a polycrystalline  $\text{SrTiO}_3$  substrate were determined using electron backscatter diffraction. This high-throughput investigation, we call combinatorial substrate epitaxy, enables the characterization of film growth on all grain orientations in a single experiment, allowing the determination of the preferred epitaxial orientation (*PEO*) of this non-isostructural film/substrate pair. Heavily-twinned rhombohedral  $\alpha\text{-Fe}_2\text{O}_3$  (hematite) grew epitaxially over the entire orientation space of the cubic perovskite substrate. Over 500 local orientation relationships (*ORs*) were investigated and more than 90% of these *ORs*, regardless of the interface plane normal, could be described using a single epitaxial *OR*:  $(0001) [10\bar{1}0]_{\text{Fe}_2\text{O}_3} \parallel (111) [1\bar{1}0]_{\text{SrTiO}_3}$ . This *OR* aligns the eutactic (nearly close-packed) planes and directions between these dissimilar crystal structures. Importantly, the growth of  $\text{Fe}_2\text{O}_3$  on a single crystalline (100)- $\text{SrTiO}_3$  results in several different orientation relationships. These results suggest that growth on high Miller-index (low-symmetry) surfaces provides more general information about the *PEO* than growth on low Miller-index (high-symmetry) surfaces. The epitaxial film growth on high Miller-index surfaces and the overwhelming observation of the eutaxial *OR* support the hypothesis that a very small number of simple crystallographic descriptors guide epitaxial film growth over all of orientation space, even for non-isostructural film/substrate pairs.

© 2013 Elsevier B.V. All rights reserved.

## 1. Introduction

Epitaxy, or the ordered growth of one crystal on another [1–4], has played a central role in a range of technological and scientific advances over the past century [1,4–8]. Surprisingly, we have a relatively crude physical understanding of what the preferred epitaxial orientation (*PEO*) is between two dissimilar solids (heteroepitaxy). The overwhelming majority of prior investigations into heteroepitaxy use single crystal substrates exposing low Miller-index, high-symmetry surfaces to the growing solid. From the point of view of interface crystallography, this work is restricted to a very narrow region of epitaxial orientation space (herein defined relative to the substrate surface normal) and focuses on what should be considered extremely special interfaces. Most models of epitaxy aim to simplify the nucleation energetics to descriptors of the geometric match between the two crystals at these special interfaces [4,5,9–13,6,14–16]. A simple question arises: does epitaxial growth on special surfaces reflect the *PEO* between two crystals in general?

Recent developments in high-throughput characterization methods, especially using electron backscatter diffraction (*EBS*D), have allowed investigations to address this question. Chatain and Galy [17] used

high-throughput *EBS*D methods to study the orientation relationship (*OR*) between micron-sized Pb crystals (crystallized from the melt) on polycrystalline Cu substrates. They found a cube-on-cube epitaxial *OR* for almost all surface orientations, despite the large lattice mismatch and preference of fcc metals to have the {111} planes parallel to the substrate surface. These observations indicated that the substrate surface normal was not a key driver in the development of the *PEO*; however, significant morphological changes occurred to the surface normal during processing, complicating the interpretation [17]. Floro et al. [18] used similar high-throughput *EBS*D methods to investigate the epitaxy of ZnO nanowires crystallized from solutions on Ag surfaces, observing only two *ORs*, a predominant one for surfaces near {111} and a secondary one for surfaces near {100} Ag. They highlighted that kinetic factors played an important role in crystallization from solution, as the nanorod density varied strongly with orientation [18]. The strongly faceted surfaces of Ag were implicated as driving the *ORs* across orientation space, as many surfaces exposed large areas of {111} terraces [18].

We have been developing a similar high-throughput method to explore growth over all epitaxial orientation space, a method we call combinatorial substrate epitaxy (*CSE*) [19]. In *CSE*, films are deposited on smoothly polished polycrystalline substrates, local orientations of both the film and substrate are mapped using *EBS*D, and the film–substrate orientation relationships (*ORs*) can be compared on a grain-by-grain basis. Using *CSE*, we investigated the epitaxial growth of anatase and

\* Corresponding author. Tel.: +1 412 268 2702; fax: +1 412 268 3113.

E-mail addresses: [paulsalvador@cmu.edu](mailto:paulsalvador@cmu.edu), [paul7@andrew.cmu.edu](mailto:paul7@andrew.cmu.edu) (P.A. Salvador).

rutile  $\text{TiO}_2$  on ferroelectric perovskites  $\text{BaTiO}_3$  [20] and  $\text{BiFeO}_3$  [19], and the epitaxial growth of complex titanates [21], over the entire range of epitaxial orientation space. Collectively those studies show two important things. First, well-prepared polycrystalline surfaces can be treated locally as single-crystal growth surfaces, which were free from microfacetting. Second, only a small number of ORs are observed in heteroepitaxy even for non-isostructural film/substrate pairs over all epitaxial orientation space; >90% (80%) of all anatase (rutile)  $\text{TiO}_2$  grains grew on  $\text{BiFeO}_3$  with the *PEO* that aligned the eutactic (nearly close-packed [22]) planes and directions of the film and substrate, regardless of the surface normal of the substrate [19]. This *PEO* was termed the eutactic OR, and epitaxial growth can be described as epitaxial growth that leads to the extension of the closest-packed networks between the film and substrate [22]. The eutactic OR was shown to be a more general descriptor than any prior interfacial descriptors based on  $\text{TiO}_2$  growth on low-index single-crystal perovskite surfaces [19] (and similar to the *PEO* of Pb microcrystals on Cu [17]).

Here, we use CSE to test the hypothesis that the eutactic OR is the *PEO* for films of hematite  $\text{Fe}_2\text{O}_3$  grown on the perovskite  $\text{SrTiO}_3$ . Hematite (isostructural with corundum) has a hexagonal close packed (hcp) network of oxygen atoms, with iron atoms filling 2/3 of the octahedral interstices. The close packed oxygen plane is  $\{0001\}$ , and the close packed direction within this plane is  $\langle 1\bar{1}00 \rangle$ .  $\text{SrTiO}_3$  has a cubic close packed (ccp) network of  $\text{SrO}_3$  atoms, with titanium atoms in 1/4 of the octahedral interstitial sites. The close packed planes are  $\{111\}$ , and the close packed directions within that plane are  $\langle 1\bar{1}0 \rangle$ . We show here that the eutactic OR is overwhelmingly the *PEO* on general surfaces, even in conditions for which it is not uniquely observed on single-crystal special interfaces [23–27]. These observations indicate the *PEO* on general surfaces is best described using 3D models of the crystal structure alignment, and that growth on general surfaces results in a smaller number of ORs than observed on low-index surfaces.

## 2. Experimental details

A polycrystalline  $\text{SrTiO}_3$  substrate was prepared using standard ceramic methods from commercial  $\text{SrTiO}_3$  powder (99.97%).  $\text{SrTiO}_3$  pellets were annealed consecutively at 900, 1360, and 1470 °C for 10, 10, and 3 h, respectively. The sintered substrates were lapped, polished, and annealed as described elsewhere (for  $\text{Fe}_2\text{O}_3$  pellets) [26]. The final pellets were approximately 2 mm thick and 8 mm in diameter. 50 nm thick  $\alpha\text{-Fe}_2\text{O}_3$  films were deposited on  $\text{SrTiO}_3$  polycrystals and commercial (100) single-crystals, as described elsewhere [26].

After deposition, an area of the film was mapped using *EBSD* [28]. Then, the film was polished away by hand using 0.3  $\mu\text{m}$  colloidal silica. Polishing was stopped when the film (which was reddish) was no longer visible on the surface of the pellet, after  $\approx 30$  s. The same area of the surface was mapped using *EBSD*. The data was processed with one iteration of a grain dilation algorithm (with a minimum grain size of 5 pixels and a grain tolerance angle of 5°) and subsequently by assigning a single average orientation to each grain (averaging the orientation of all points within the identified grain). The orientation relationships between film/substrate pairs were determined using software and methods described in Ref. [19].

## 3. Results and discussion

Inverse pole-figure (*IPF*) maps taken from the same area on the polycrystalline specimen (imaged in plan view) are shown in Fig. 1(a) for the film and Fig. 1(b) for the substrate after film removal. The colors used in *IPF* maps represent the orientation of each point on the map relative to the surface normal (the color keys are given as stereographic triangles in the insets). The outlined regions in each map represent three pairs of film and substrate grains, simply as guides. In general, each substrate grain nucleates a small set of film grains, usually corresponding to two distinct twin orientations (discussed below). In

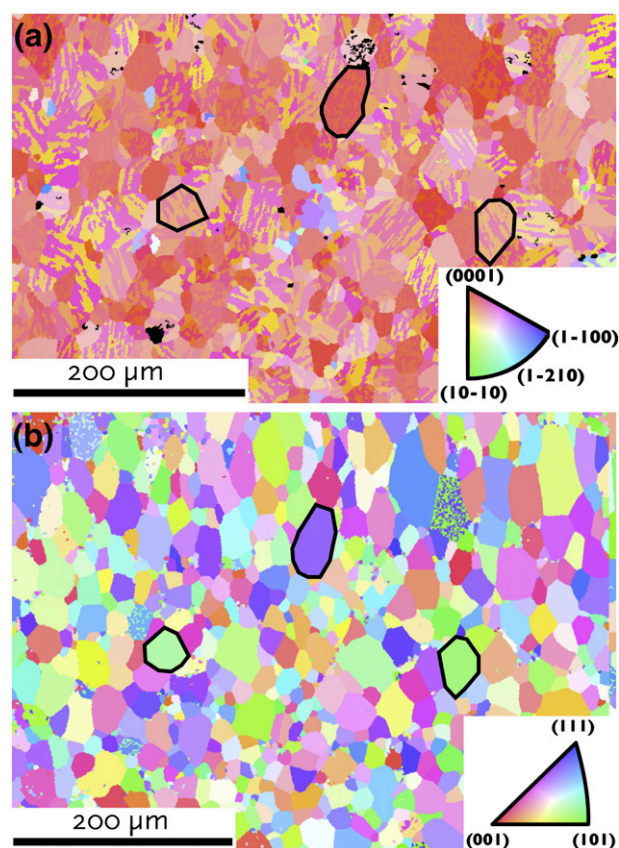


**Fig. 1.** Inverse pole-figure *EBSD* maps of the same area of (a) a 50 nm hexagonal  $\text{Fe}_2\text{O}_3$  film on (b) a polycrystalline cubic  $\text{SrTiO}_3$  substrate. The color-key of the orientations are given in the insets as standard stereographic triangles for the specific crystal systems. Outlined areas represent the same area of the sample.

traditional epitaxy on single crystal substrates, these regions are often called variants and represent degenerate orientations that are crystallographically identifiable owing to the different symmetries of the film and substrate. In some regions, areas containing individual pixels assigned to widely varying orientations were cleaned up and colored black in the *IPF* map. Even film grains that appear at this scale to be a single color, actually have multiple film grains (i.e., twins) as determined by the *EBSD* software at higher resolution: one such high-resolution *IPF* map is shown as the inset in Fig. 2. Here, small regions (which occupy low area fractions) of differently colored orientations (some of which arise from poor image quality in the region) from the matrix can be observed.

To determine the *PEO*, we calculated (for 501 identified film/substrate pairs on 117 substrate grains) the angle between  $[111]_{\text{sub}}$  and  $[0001]_{\text{film}}$ , corresponding to the normal to the eutactic planes of each solid (the out-of-plane OR). We also calculated the angle between  $[1\bar{1}0]_{\text{sub}}$  and  $[10\bar{1}]_{\text{film}}$  (for these same pairs), corresponding to the close-packed direction in the eutactic plane (the in-plane OR). The average angle (standard deviation) between  $[111]_{\text{sub}}$  and  $[0001]_{\text{film}}$  is 4.2° (6.5°), while the average angle between  $[1\bar{1}0]_{\text{sub}}$  and  $[10\bar{1}]_{\text{film}}$  is 3.0° (5.2°). The angular distributions are given in Fig. 2, where each distribution is plotted versus a pair ID number, which is ordered from minimum to maximum angle for each distribution. More than 450 of the 501 film/substrate pairs (>90%) are within 5° of the eutactic OR for both the in-plane and out-of-plane ORs. Slightly above the Pair ID number 461, in both distributions, the misorientation angles become much larger than 5°. All points lying in this region are considered outliers to

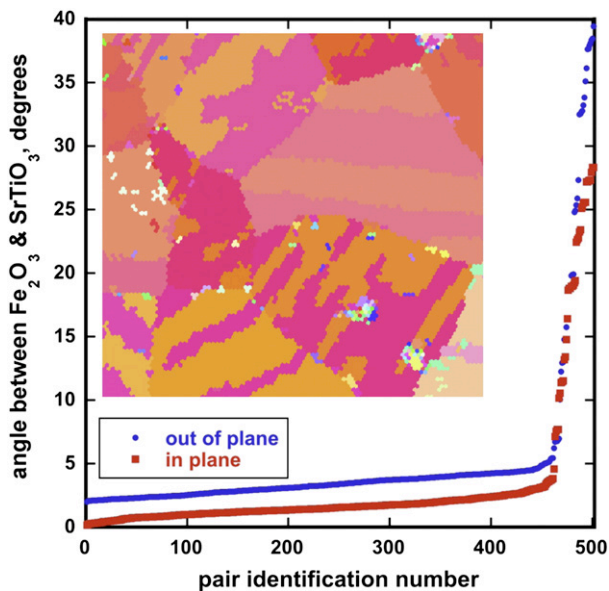


Fig. 2. Plot of the angle of misorientation between the film [0001] and the substrate [111] (out-of-plane, blue circles) and the film  $[1\bar{1}00]$  and substrate  $[1\bar{1}0]$  (in-plane, red squares). Inset: a high resolution IPF map of another region of the  $\text{Fe}_2\text{O}_3$  film grains (the horizontal width is  $46\ \mu\text{m}$ ).

the primary distribution, and represent  $\approx 5$ – $10\%$  of the population. We did not attempt any systematic investigation into these outliers except to ensure these were correctly assigned as non-eutactic orientations in the population. That there are other orientations is not surprising given the complexity of film growth; that there is less than  $\approx 10\%$  that adopt non-eutactic orientations over all orientation space is surprising. Using only the first 461 pairs, the average angle (standard deviation) between  $[111]_{\text{sub}}$  and  $[0001]_{\text{film}}$  is  $2.6^\circ$  ( $1.0^\circ$ ) and between  $[1\bar{1}0]_{\text{sub}}$  and  $[10\bar{1}0]_{\text{film}}$  is  $1.6^\circ$  ( $0.7^\circ$ ).

These observations strongly support the hypothesis that the eutactic OR is the PEO, similar to that observed for anatase and rutile  $\text{TiO}_2$  on perovskites [19]. A small average rotation (of a few degrees) between the networks can arise experimentally from the remounting of the sample, during which the alignment is done visually. Inherent uncertainty in the absolute assignment of angles in the cleaned EBSD data [19] should cause scatter around the average orientation values (of at most  $1^\circ$ ). The distribution of points for the first 461 points is within these levels of uncertainty. Small rotations between epitaxial networks (on the order of several degrees) can also arise from misfit accommodation mechanisms, which should be a function of the local orientation and interface plane, and therefore would vary from grain to grain [9,29,10,13,6,16,30]. It should be noted that the local epitaxial misorientation sometimes varied significantly between film grains on the same substrate grain, indicating that at least a portion of the misorientation value has to do with crystallographic accommodation at the interface. Overall, we did not attempt to establish which of these factors dominate the angular difference between the eutactic networks; the primary goal was to demonstrate that they are aligned. It is possible to improve the methodology to determine more clearly the relative contributions of experimental and symmetry-related uncertainties, as well as misfit accommodation effects.

For all substrate grains, at least two different film orientations were observed, representing twin domains. All twins were determined to have a misorientation corresponding to a  $60^\circ$  rotation about [0001], a common misorientation in corundum twins [31]. The two colors observed in the IPF map for the film grains on any individual substrate grain simply reflect how the normal to the surface is affected by a  $60^\circ$

rotation about [0001], which is inclined to the surface. The yellow/purple pairs in the IPF have the most color contrast, but all grains have similar twin structures. The orientations of more than half of the twin boundary-surface intersections were consistent with a (0001) habit plane for the twin boundary, consistent with predicted low energy basal twins in corundum (see [31,32] and references therein). Because of the meandering shape of the twins, other boundary orientations are needed to bound the grain.

It is noted that the use of multiple film/substrate pairs for each substrate grain affects the statistical analysis of the data. Because each substrate grain resulted in an average of  $\approx 4$  calculated ORs, each additional film grain doesn't represent an entirely unique substrate-grain pair. It should also be noted that the number density of eutaxial grains, described here, is likely to be lower than the area fraction of eutaxial grains. The size of the eutaxial grains is always much larger than the non-eutaxial grains. Therefore, the values reported here are reasonable representations of the population and convey the overwhelming preference for the eutactic OR.

The wide range of colors observed in the substrate IPF color map in Fig. 1(b) indicates that surface orientations over the entire epitaxial orientation space were used in the investigation of the PEO. This is further demonstrated in Fig. 3(b), where the orientations of specific grains used in the calculations are plotted within the stereographic triangle. On the other hand, the IPF map for the film contains colors that are mainly shades of red, orange, pink, and yellow, colors representing film grains located near the (0001) orientation. This indicates that the film grains are not distributed throughout orientation space, as observed in Fig. 3(a). This arises simply from differences in the angular range of orientation space owing to symmetry differences in the crystal classes. In the cubic system, the maximum angular spread between non-equivalent directions is  $54.7^\circ$ , while in the hexagonal system it is  $90^\circ$ . The compression of the film data near [0001] reinforces the eutaxial growth mode, since the films follow the substrate orientations closely. Also note that we found the outlier grains to be uniformly distributed throughout the orientation space, but still compressed toward the (0001) orientation, indicating that the outliers are also orientated in space relative to the substrate, i.e., they are also epitaxial.

Across the entirety of epitaxial orientation space we find that the eutactic OR is the simplest descriptor for film growth (regardless of the substrate surface normal), and should be considered the PEO of  $\alpha\text{-Fe}_2\text{O}_3$  on  $\text{SrTiO}_3$ . This eutactic OR matches observations of epitaxial growth of  $\alpha\text{-Fe}_2\text{O}_3$  films on (0001)  $\text{Al}_2\text{O}_3$  [33–35,26] and (001)  $\text{TiO}_2$  [36] single crystal substrates. The eutactic OR was also observed for epitaxial  $\alpha\text{-Fe}_2\text{O}_3$  on perovskite substrates: (111)  $\text{SrTiO}_3$  [26] and (001)  $\text{LaAlO}_3$  [27]. However, Chen et al. [23,24] reported that hematite growth (using similar conditions to those here) on (001)  $\text{SrTiO}_3$  surfaces resulted in polycrystalline films. The latter work suggests that our films should be polycrystalline near the (001) orientations, but we do

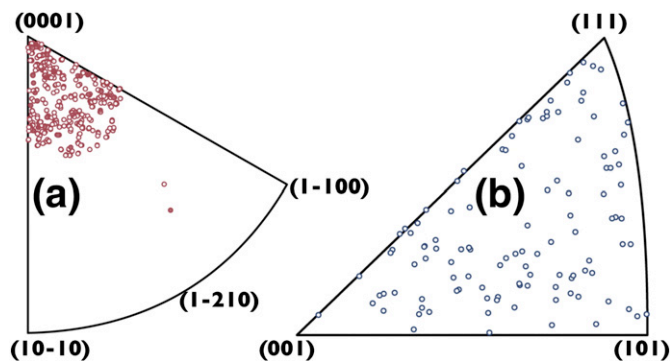
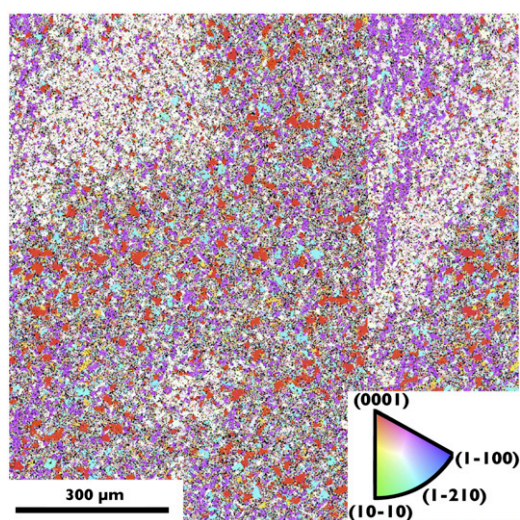


Fig. 3. Orientations of the grains used for orientation calculations, and shown in Fig. 1, plotted in the standard stereographic triangle for (a) the film and (b) the substrate.



**Fig. 4.** IPF map of an  $\text{Fe}_2\text{O}_3$  film on a  $\text{SrTiO}_3(001)$  substrate. Five distinct colors – red, purple, white, cyan, and yellow – have considerable area fractions in the overall population (see Table 1).

not observe this for growth on polycrystalline  $\text{SrTiO}_3$ . To understand how observations on polycrystals compare to those on single crystals, we deposited a film on a (001)  $\text{SrTiO}_3$  single crystal.

Fig. 4 shows an IPF map for an  $\text{Fe}_2\text{O}_3$  film grown on a (100)-oriented  $\text{SrTiO}_3$  single crystal, and it is clearly polycrystalline (similar to Chen et al. [23,24]). (Under identical growth conditions we found epitaxial films grew on (111)  $\text{SrTiO}_3$  single crystals [26].) While there are colors from a wider region of orientation space for the film on the (001) single crystal (compared to Fig. 1(a)), there are only a small number of distinct colors that dominate the population. The population was binned into five distinct color bins (orientations) and their area fractions were determined. These values are given in Table 1. The purple and white partitions represent the two twin orientations of the eutactic OR (we verified that both the in-plane and out-of-plane eutactic directions were aligned). Even though the film is polycrystalline on this single crystal surface, the eutactic OR is still the largest single OR in the population. More than 1/3 ( $\approx 37.4\%$ ) of the area fraction corresponds to grains with the eutactic OR, supporting that this is the PEO.

A combination of growth and substrate surface parameters determines nucleation kinetics, which are difficult to compare completely between different growth environments. It is likely that one could isolate conditions where several of these five orientations could be completely isolated on (100)  $\text{SrTiO}_3$  (or other perovskites), in particular the eutactic OR. Indeed, the observations by Wang et al. [27] support this assertion, as they were able to obtain eutaxial ( $10\bar{1}2$ )-oriented  $\alpha\text{-Fe}_2\text{O}_3$  on (001)  $\text{LaAlO}_3$ . Differences in the growth parameters are also likely the reason we observe eutaxial  $\alpha\text{-Fe}_2\text{O}_3$  on (111)  $\text{SrTiO}_3$ , while Gich et al. [25] found epitaxial  $\epsilon\text{-Fe}_2\text{O}_3$  on (111)  $\text{SrTiO}_3$  single crystals. Our growth conditions favor hematite formation on all grains, and the surfaces of the polycrystal more strongly favor the eutaxial PEO as compared to

the (100) single crystal. The latter observation is likely associated with a less-degenerate nucleation landscape owing to lower symmetry or more surface defects on the polycrystal.

Describing the PEO using the typical geometrical arguments of structural matching at special interfaces is nearly impossible. First, we used 117 differently orientated grains to generate the 501 film observations. If we described the epitaxial growth relative to these sample normal vectors, we would need 117 individual descriptors, and would have to write even more epitaxial relationships (at least twice that since all grains are twinned). It should be noted that in typical single-crystal investigations using different low Miller-index orientations, the individual descriptors are used on different orientations. It seems reasonable that this level of expected complexity would be enough to drive growth studies toward the special low-index surfaces. However, these observations indicate that one simple descriptor covers 95% of our observations. Second, on the high-symmetry low Miller-index surfaces, where conventional descriptions are expected to hold, we observe polycrystalline growth, indicating that this special surface does not accurately represent growth of  $\text{Fe}_2\text{O}_3$  on a general  $\text{SrTiO}_3$  surface. Nevertheless, the eutactic OR is still the largest single OR in the population (by area fraction).

The use of polycrystalline substrates and EBSD mapping for determining the PEO represents a significant technical step forward. CSE allows for high throughput studies of film growth on high and low index orientations. Using CSE, a single film deposition results in hundreds of individual substrate/film pairs. Each of these pairs can be thought to represent a single growth experiment. The observations made here using CSE, and previously for  $\text{TiO}_2$  growth on  $\text{BiFeO}_3$  [19], support the assertion that one simple descriptor describes the PEO of corundum, anatase, and rutile films on perovskite substrates: the PEO aligns the eutactic networks between the film and the substrate (the eutactic OR). Surprisingly, on low Miller-index surfaces, other ORs compete better with the eutaxial grains than on the high Miller-index surfaces, thereby confusing the identification of the PEO on low Miller-index surfaces.

#### 4. Conclusions

The preferred epitaxial orientation (PEO) of a  $\text{Fe}_2\text{O}_3$  film, grown using pulsed laser deposition, on a polycrystalline  $\text{SrTiO}_3$  substrate was determined by establishing the grain-by-grain orientation relationships using electron backscatter diffraction (EBSD). Using this high-throughput methodology, we call combinatorial substrate epitaxy (CSE), over 500 local orientation relationships (ORs) were investigated and more than 90% of these ORs, regardless of the interface plane normal, could be described using a single epitaxial OR:  $(0001)_{\text{Fe}_2\text{O}_3} \parallel (10\bar{1}0)_{\text{SrTiO}_3}$ .

This OR aligns the eutactic (nearly close-packed) planes and directions between these dissimilar crystal structures.  $\text{Fe}_2\text{O}_3$  films on a single crystalline (100)- $\text{SrTiO}_3$  display several different orientation relationships; nevertheless, the eutaxial OR accounts for the largest area fraction (more than 1/3). These results suggest that growth on high Miller-index (low-symmetry) surfaces provide more general information about the PEO than growth on low Miller-index (high-symmetry) surfaces. The epitaxial film growth on high Miller-index surfaces and the overwhelming observation of the eutaxial OR supports the hypothesis that a very small number of simple crystallographic descriptors guide epitaxial film growth over all of orientation space, even for non-isostructural film/substrate pairs.

#### Acknowledgments

The authors acknowledge the National Science Foundation grant DMR 1206656 for the support of this research.

**Table 1**

Summary of the area fraction of points falling into the five color bins from the map in Fig. 4. The total number of points falling into one of the five color bins is 257,004, representing a 60.4% fraction of the total number of points.

	Orientation	Number of points	Area fraction
Red	(0001)	45,072	0.105
Cyan	(1 $\bar{2}$ 00)	37,497	0.088
Purple	(10 $\bar{1}$ 2)	55,640	0.130
White	(1 $\bar{2}$ 13)	103,881	0.244
Yellow	(1 $\bar{1}$ 14)	14,914	0.035
All data		425,917	1.000

## References

- [1] L. Royer, *Bull. Soc. Fr. Minéral.* 51 (1928) 7.
- [2] L. Royer, *Bull. Soc. Fr. Minéral.* 77 (1954) 1004.
- [3] D.W. Pashley, *Adv. Phys.* 5 (1956) 173.
- [4] D.W. Pashley, *Adv. Phys.* 14 (1965) 327.
- [5] J.L. Kenty, J.P. Hirth, *Surf. Sci.* 15 (1969) 403.
- [6] C.J. Palmstrom, *Annu. Rev. Mater. Sci.* 25 (1995) 389.
- [7] M. Ohring, *Materials Science of Thin Films*, Academic Press, 2001.
- [8] M.A. Herman, W. Richter, H. Sitter, *Epitaxy: Physical Principles and Technical Implementation*, Springer, 2004.
- [9] J.W. Matthews, A.E. Blakeslee, *J. Cryst. Growth* 27 (1974) 118.
- [10] J.H. Van Der Merwe, *Phil. Mag.* 45 (1982) 127.
- [11] R.C. Pond, *Crit. Rev. Solid State Mater. Sci.* 15 (1989) 441.
- [12] H.J. Fecht, *Phil. Mag. Lett.* 60 (1989) 81.
- [13] M. Aindow, R.C. Pond, *Phil. Mag.* 63 (1991) 667.
- [14] D.E. Hooks, T. Fritz, M.D. Ward, *Adv. Mater.* 13 (2001) 227.
- [15] C.P. Flynn, J.A. Eades, *Thin Solid Films* 389 (2001) 116.
- [16] J. Narayan, B.C. Larson, *J. Appl. Phys.* 93 (2003) 278.
- [17] D. Chatain, D. Galy, *J. Mater. Sci.* 41 (2006) 7769.
- [18] J. Floro, J. Michael, L. Brewer, J. Hsu, *J. Mater. Res.* 25 (2010) 1352.
- [19] Y. Zhang, A.M. Schultz, L. Li, H. Chien, P.A. Salvador, G.S. Rohrer, *Acta Mater.* 60 (2012) 6486.
- [20] N.V. Burbure, P.A. Salvador, G.S. Rohrer, *J. Am. Ceram. Soc.* 93 (2010) 2530.
- [21] S. Havelia, S. Wang, K.R. Balasubramaniam, A.M. Schultz, G.S. Rohrer, P.A. Salvador, *CrystEngComm* 15 (2013) 5434.
- [22] M. O'Keeffe, *Acta Crystallogr. A* 33 (1977) 924.
- [23] Y.S. Chen, B. Chen, B. Gao, F.F. Zhang, Y.J. Qiu, G.J. Lian, L.F. Liu, X.Y. Liu, R.Q. Han, J.F. Kang, *Appl. Phys. Lett.* 97 (2010) 262112.
- [24] Y. Chen, G. Lian, G. Xiong, T. Venkatesan, *Appl. Phys. Lett.* 98 (232513) (2011) 1.
- [25] M. Gich, J. Gazquez, A. Roig, A. Crespi, J. Fontcuberta, J.C. Idrobo, S.J. Pennycook, M. Varela, V. Skumryev, M. Varela, *Appl. Phys. Lett.* 96 (112508) (2010) 1.
- [26] A.M. Schultz, P.A. Salvador, G.S. Rohrer, *Chem. Commun.* 48 (2012) 2012.
- [27] Z. Wang, R. Viswan, B. Hu, V.G. Harris, J.-F. Li, D. Viehland, *Phys. Status Solidi (RRL)* 6 (2012) 89.
- [28] A.M. Schultz, Y. Zhang, P.A. Salvador, G.S. Rohrer, *ACS Appl. Mater. Interfaces* 3 (2011) 1562.
- [29] J.W. Matthews, A.E. Blakeslee, *J. Cryst. Growth* 29 (1975) 273.
- [30] R.C. Pond, X. Ma, J.P. Hirth, T.E. Mitchell, *Phil. Mag.* 87 (2007) 5289.
- [31] T.E. Mitchell, *Dislocations in Ceramics*, in: R. Riedel, I.-W. Chen (Eds.), *Ceramics Science and Technology, Materials and Properties, Volume 2*, Wiley-VCH Verlag GmbH & Co. KGaA, Weinheim, Germany, 2008, <http://dx.doi.org/10.1002/9783527631735.ch9>.
- [32] A. Marinopoulos, S. Nufer, C. Elsasser, *Phys. Rev. B* 63 (2001) 165112.
- [33] T. Fujii, D. Alders, F.C. Voogt, T. Hibma, B.T. Thole, G.A. Sawatzky, *Surf. Sci.* 366 (1996) 579.
- [34] Y.J. Kim, Y. Gao, S.A. Chambers, *Surf. Sci.* 371 (1997) 358.
- [35] I. Yamaguchi, T. Manabe, T. Kumagai, W. Kondo, S. Mizuta, *Thin Solid Films* 365 (2000) 36.
- [36] J.R. Williams, C.M. Wang, S.A. Chambers, *J. Mater. Res.* 20 (2005) 1250.